

# In Vivo and In Vitro Dynamics of Undifferentiated Embryonic Cell Transcription Factor 1

Christina Galonska,<sup>1,2,3</sup> Zachary D. Smith,<sup>1,2,3</sup> and Alexander Meissner<sup>1,2,3,\*</sup>

<sup>1</sup>Broad Institute of MIT and Harvard, Cambridge, MA 02142, USA

<sup>2</sup>Harvard Stem Cell Institute, Cambridge, MA 02138, USA

<sup>3</sup>Department of Stem Cell and Regenerative Biology, Harvard University, Cambridge, MA 02138, USA

\*Correspondence: [alexander\\_meissner@harvard.edu](mailto:alexander_meissner@harvard.edu)

<http://dx.doi.org/10.1016/j.stemcr.2014.01.007>

This is an open-access article distributed under the terms of the Creative Commons Attribution-NonCommercial-No Derivative Works License, which permits non-commercial use, distribution, and reproduction in any medium, provided the original author and source are credited.

## SUMMARY

Pluripotent stem cells retain the ability to differentiate into the three germ layers and germline. As a result, there is a major interest in characterizing regulators that establish and maintain pluripotency. The network of transcription factors continues to expand in complexity, and one factor, undifferentiated embryonic cell transcription factor 1 (UTF1), has recently moved more into the limelight. To facilitate the study of UTF1, we report the generation and characterization of two reporter lines that enable efficient tracking, mapping, and purification of endogenous UTF1. In particular, we include a built-in biotinylation system in our targeted locus that allows efficient and reliable pulldown. We also use this reporter to show the dynamic regulation of *Utf1* in distinct stem cell conditions and demonstrate its utility for reprogramming studies. The multipurpose design of the reporter lines enables many directions of future study and should lead to a better understanding of UTF1's diverse roles.

## INTRODUCTION

Self-renewal and the potential to differentiate into any cell type are the defining features of pluripotent stem cells (PSCs). Maintaining the cells in this unique state is a carefully regulated process that requires the coordinated interaction of multiple transcription factors (TFs) and epigenetic regulators (Jaenisch and Young, 2008). A subset of core pluripotency factors, including OCT4, SOX2, and NANOG, have been the focus of many studies, and their target loci and protein interaction partners have been reported (Apostolou et al., 2013; de Wit et al., 2013; Jaenisch and Young, 2008; Kim et al., 2008). Several other genes have been linked to the regulation of pluripotency, including *Sall4*, *Esrrb*, *Tbx3*, *Tcl1*, and *Utf1* (Ng and Surani, 2011). Undifferentiated embryonic cell transcription factor 1 (UTF1) was one of the initial 24 factors selected by Takahashi and Yamanaka (2006) to screen for cellular reprogramming to pluripotency, and was later shown to increase reprogramming efficiency when included with the four core factors (Zhao et al., 2008). *Utf1* was first classified as a transcriptional coregulator expressed in embryonic stem cells (ESCs), embryonic carcinoma cells, cells of the germline, and teratocarcinoma cells (Okuda et al., 1998). Subsequent knockdown studies of *Utf1* suggested that it plays a regulatory role in cellular differentiation by controlling the chromatin organization at its associated target sites, many of which are cobound by the core pluripotency factors OCT4, SOX2, and NANOG (Kooistra et al., 2010). More recent reprogramming studies have shown that *Utf1* undergoes early chromatin dynamics that pre-

cede its transcriptional activation (Koche et al., 2011), and based on single-cell, time-course expression analysis, it appears that *Utf1* is expressed in a restricted population of reprogramming cells, making it a potential marker to detect early, successful reprogramming events (Buganim et al., 2012).

Another recent study reported that UTF1 and PRC2 compete for the same target sites, thereby balancing the deposition of H3K27me3 at bivalent genes, which in turn may be essential to control the induction of the respective genes upon exit of pluripotency (Jia et al., 2012). In line with that, *Utf1* knockout cells showed less effective differentiation. As a complementary mechanism, UTF1 recruits the DCp1a subunit, a component of the mRNA-decapping machinery, to these same bivalent genes (Jia et al., 2012). Therefore, UTF1 has been proposed to serve a dual role in preventing excessive binding of the PRC2 complex to bivalent genes while simultaneously facilitating the tagging of mRNA from leaky repression for degradation. Interestingly, Marks et al. (2012) showed that *Utf1* is one of the most downregulated genes upon culture under the inhibitor-based, serum-free 2i/leukemia inhibitory factor (LIF) condition (i.e., dual inhibition of MEK1 and GSK3 by small-molecule inhibitors), which maintain pluripotent cells in a more homogeneous undifferentiated state (Ying et al., 2008). *Utf1*'s tightly regulated expression during reprogramming and within pluripotent cells under conventional serum/LIF conditions, in addition to its potential role as a transient suppressor of lineage-specifying genes, support the growing interest in this factor.

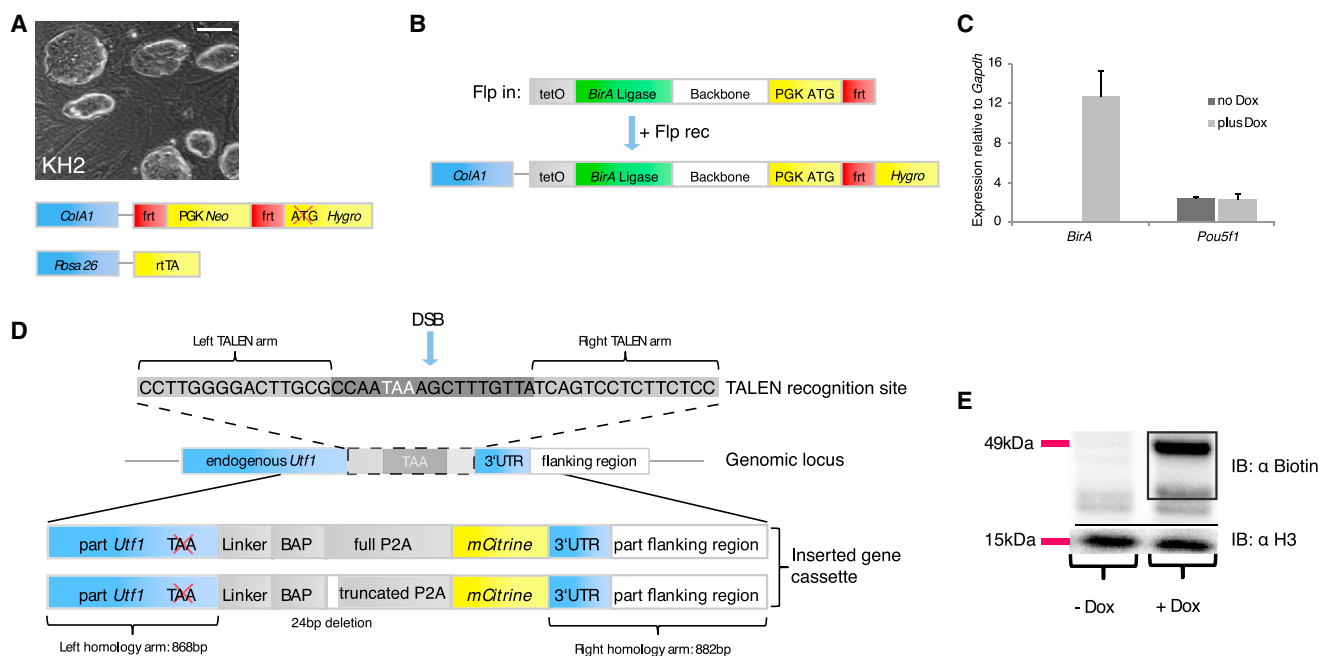


**Figure 1. Generation of *Utf1* Reporter ESC Lines**

(A) Top: bright-field image of KH2 mouse ESCs. Scale bar, 100  $\mu$ m. Bottom: the cells contain an frt-flanked neomycin (Neo) cassette and a hygromycin (Hygro) cassette missing the start codon downstream of the *ColA1* locus, as well as the rtTA coding sequence downstream of the ubiquitously expressed *Rosa26* locus.

(B) The Flp in system enables Flp recombinase (Flp rec)-mediated targeting of the *ColA1* locus. Integration of our tetO-BirA cassette can be selected by hygromycin resistance and removes the neomycin resistance cassette (A, bottom).

(C) Quantitative RT-PCR for *BirA* and *Oct4* (*Pou5f1*) expression relative to *Gapdh* expression with or without doxycycline. Addition of 2  $\mu$ g/ml doxycycline for 24 hr induces notable expression of the BirA biotin ligase. Whiskers show 1 SD for n = 3 independent experiments.

(D) TALEN-based strategy to target the endogenous *Utf1* locus. Targeting arms (15 base pairs) match the C-terminal end of the endogenous *Utf1* sequence. The double-strand break (DSB) is induced within the 17 bp region between the recognition sites, harboring the stop codon (highlighted in white). Successful targeting couples UTF1 to a short flexible linker, BAP, a full/truncated P2A sequence, and the fluorescent marker mCitrine.

(E) Western blot showing successful biotinylation of endogenous UTF1 after addition of 2  $\mu$ g/ml doxycycline for 48 hr. The box indicates the typical two bands observed for UTF1.

See also Figure S1.

Here we report the generation and characterization of *Utf1* reporter cell lines, and highlight their utility and faithful expression with several relevant examples.

## RESULTS

### Generation of Endogenous *Utf1* Reporter ESC Lines

Our goal was to create versatile reporter lines for *Utf1* that would facilitate the investigation of its role in pluripotency, differentiation, and reprogramming. To this end, we used the KH2 ESC line (Figure 1A), which contains an frt-flanked resistance cassette downstream of the *ColA1* locus and the rtTA open reading frame downstream of the *Rosa26* locus (Beard et al., 2006). We introduced a tetracycline-responsive *E. coli* BirA biotin ligase (Barker and Campbell, 1981)

into the collagen locus using flp recombinase (Figure 1B). As shown in Figure 1C, we observed induced expression of the ligase within 24 hr after adding doxycycline to the media. This new cell line (KH2-BirA) was then used to target the endogenous *Utf1* locus with two distinct constructs that tied its expression to an mCitrine reporter (Figure 1D). One construct contains the full-length P2A sequence, which signals for cotranslational cleavage between UTF1 and the reporter, and the other contains a truncated version lacking the first eight amino acids (Figure S1A available online) to negate this cleavage and function as a fusion protein. The full-length P2A sequence allows for the generation of separate mCitrine protein and reports transcript levels, while the truncated version serves as an effective proxy for protein level and localization. Finally, the biotin acceptor peptide (BAP) enables efficient

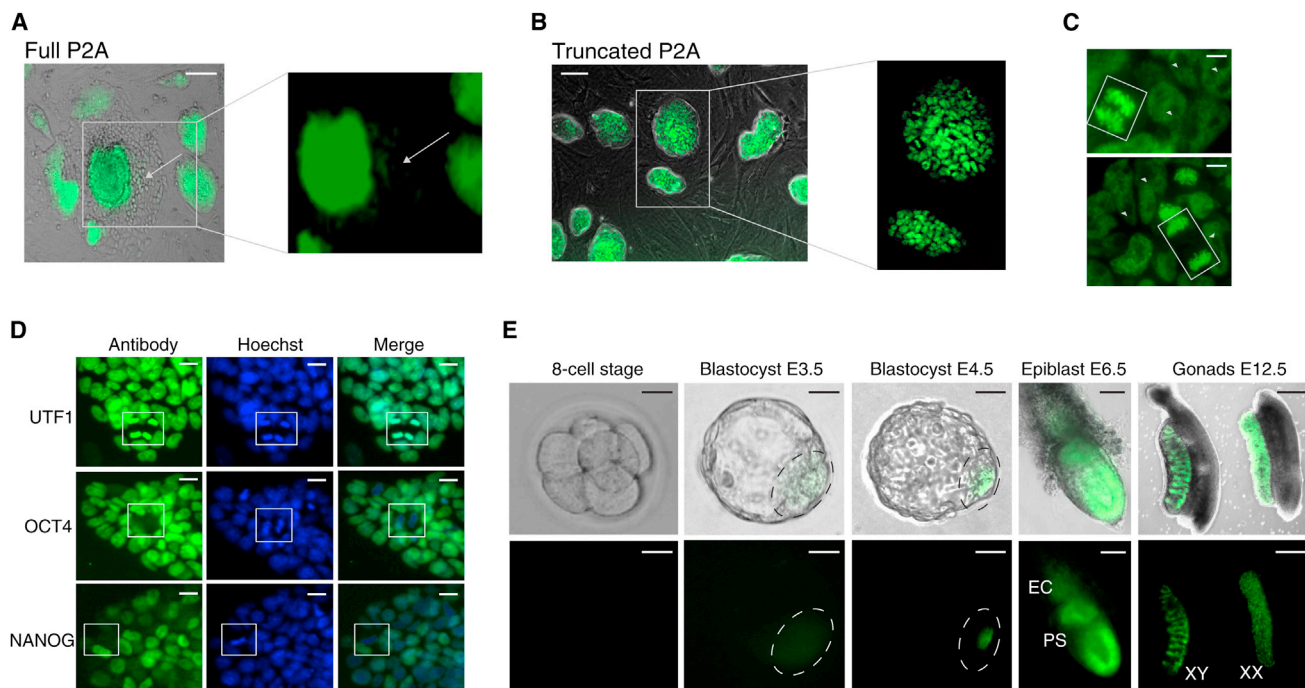


**Figure 2. In Vitro and In Vivo Characterization of the *Utf1* Reporter Lines**

(A) The *Utf1* cleavage line CHG2.4 contains a full P2A sequence, resulting in the cleavage of the mCitrine during translation. The white arrow indicates differentiated cells, which are negative for the reporter. Scale bar, 100  $\mu$ m.

(B) The *Utf1* fusion line CHG1.7 harbors a truncated P2A sequence, resulting in a UTF1-mCitrine fusion. UTF1 is exclusively located in the nucleus. Scale bar, 100  $\mu$ m.

(C) UTF1 remains associated with chromatin throughout mitosis. The white box indicates UTF1 chromatin association during mitosis (anaphase). Arrowheads indicate nucleoli. Scale bar, 10  $\mu$ m.

(D) Immunostaining for UTF1, OCT4, and NANOG. White boxes indicate dividing cells. Only UTF1 stays associated with the chromatin throughout mitosis, and NANOG and OCT4 are dissociated. Scale bar, 20  $\mu$ m.

(E) In vivo characterization of the *Utf1* cleavage line. *Utf1* shows no detectable expression at the early cleavage stages, low expression in the early blastocyst (E3.5), and higher expression in the late blastocyst (E4.5). The highest expression is observed in epiblast stage (E6.5) embryos and in primordial germ cells (PGCs) at E12.5. EC, ectoplacental cone; PS, primitive streak. Scale bars, 25  $\mu$ m (eight-cell stage, blastocyst E3.5, blastocyst E4.5), 50  $\mu$ m (epiblast E6.5), and 200  $\mu$ m (gonads E12.5). Exposure times are consistent among the different images.

See also [Figure S2](#) and [Movies S1](#) and [S2](#).

in vivo tagging and purification of endogenous UTF1 ([Figure 1E](#)). To facilitate homologous recombination, we used transcription activator-like effector nucleases (TALENs) ([Ding et al., 2013](#)) and obtained 97.5% heterozygous and 2.5% homozygous clones for the cleavage construct, and 100% heterozygous clones for the fusion construct in a single round of targeting each. For both sets, we expanded  $\sim$ 80 mCitrine-positive clones, validated the correct targeting, and then selected two representative lines (CHG1.7 [heterozygous fusion allele] and CHG2.4 [homozygous cleavage allele]) for subsequent characterizations. To test for the presence of any off-target integration sites, we performed 5'RACE against mCitrine for both the CHG1.7 and CHG2.4 lines. Sequencing of the final PCR product suggested only a single and correct integration into the *Utf1* locus ([Figures S1B](#) and [S1C](#)).

### In Vitro and In Vivo Characterization of the *Utf1* Reporter Lines

The reporter lines CHG1.7 and CHG2.4 both showed an abundant presence of UTF1 in undifferentiated mouse ESCs ([Figures 2A](#) and [2B](#)). UTF1 is predominantly localized in the nucleus but is excluded from nucleoli, and exhibits a tight association with chromatin throughout mitosis ([Figures 2B](#) and [2C](#)). This observation is in line with a previous report of UTF1 binding DNA with as tight an affinity as the core histone H2A ([van den Boom et al., 2007](#)). These binding features are very distinct from other TFs, including OCT4 and NANOG, which are not associated with DNA throughout mitosis ([Figure 2D](#)). To further assess the reporter in vivo, we generated chimeric mice from the cleavage line CHG2.4 and isolated pre- and postimplantation embryos from males exhibiting germline contribution

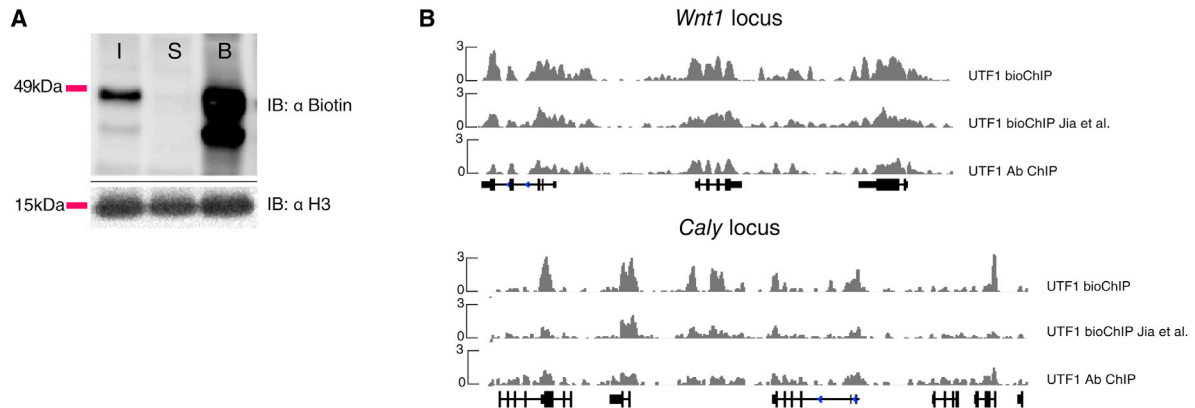


### Figure 3. Generation of High-Quality DNA-Binding Maps Using Doxycycline-Inducible Biotinylation

(A) Western blot analysis confirms that streptavidin pulldown of biotinylated UTF1 is highly sensitive and specific. I, input material; S, supernatant, input material after streptavidin pulldown; B, streptavidin-bound fraction after reverse crosslinking.

(B) Representative enrichment tracks for the UTF1-bioChIP in this study, the UTF1-bioChIP by Jia et al. (2012), and the UTF1 antibody ChIP (this study) across the *Wnt1* and *Caly* loci.

See also Figure S3.

(Figures 2E and S2A). We find that UTF1 is not detectable during the early cleavage stages and is detectable only at low levels in embryonic day 3.5 (E3.5) blastocyst, but becomes clearly visible at the later blastocyst stage (E4.5), specifically within the inner cell mass (ICM) (Figure 2E). Postimplantation, we observe strong signal in the embryonic and extraembryonic tissues of the E6.5 epiblast, but little or no fluorescence by E8.5. However, *Utf1* becomes specifically reexpressed in the gonads of E12.5 embryos, marking the primordial germ cells (PGCs) after entering the gonadal ridge (Figure 2E). Generally, expression of *Utf1* is absent in adult tissues (Figure S2B). As in mouse, *UTF1* becomes rapidly repressed upon differentiation of human ESCs, although it is expressed at much lower initial levels (Figure S2C). Taken together, these results confirm that our reporter lines faithfully track UTF1 dynamics and localization in vitro and in vivo.

### Generation of High-Quality DNA-Binding Maps Using Doxycycline-Inducible Biotinylation

In addition to our fluorescent reporter system, we introduced the BAP sequence, which in combination with the doxycycline-inducible BirA biotin ligase enables controlled biotinylation of the endogenous protein. The subsequent streptavidin-mediated pulldown of the biotinylated protein showed high efficiency and specificity (Figure 3A). Notably, a comparison between results from our UTF1-bioChIP-seq approach and previously published data for an ectopic *Utf1*-BAP construct (Jia et al., 2012), as well as conventional antibody ChIP-seq done in our lab, shows that the endogenous/inducible system works most efficiently. Both the

published bioChIP (N-terminal tag) and our biotin-based (C-terminal tag) approach showed a high overall correlation and exhibited an improved resolution compared with the conventional antibody ChIP (Figure 3B). However, our endogenous biotinylation system exhibited an improved signal-to-noise ratio as compared with the ectopically expressed *Utf1*-BAP construct, which is in competition with endogenous protein for available binding sites (Figure S3). In addition to improved signal, the effective labeling of most UTF1 molecules enabled us to reduce the cellular starting material from the conventional 5–10 million-cell input used for conventional TF ChIP to as little as 1–3 million cells. Tagging the endogenous locus of any TFs using the TALEN or CRISPR/Cas9 strategy in the KH2-BirA lines therefore provides a general tool for efficient mapping of TFs in mouse ESCs and their derivatives. This is a more cost-effective and reproducible approach than antibody-based strategies, particularly for many of the factors that do not have commercially available, ChIP-grade antibodies.

### UTF1 Is a Sensitive and Highly Specific Marker for Serum/LIF versus 2i Pluripotent Cells

Mouse ESCs are generally cultured in Dulbecco's modified Eagle's medium (DMEM) supplemented with serum and LIF (Ying et al., 2003). Alternatively, ESCs can be grown in serum-free conditions in the presence of two small-molecule inhibitors (2i): PD0325901 (MEK inhibitor) and CHIR99021 (GSK3 $\beta$  inhibitor) (Ying et al., 2008). The transcriptional and epigenomic profiles of these 2i ESCs are very distinct from those of cells cultured under serum/LIF conditions (Marks et al., 2012). Notably, switching cells from serum/LIF to 2i for eight passages resulted in



a 10-fold downregulation of *Utf1*. To more closely inspect the dynamics of *Utf1* expression when pluripotency culture conditions were changed, we utilized our CHG1.7 reporter line to track UTF1 protein levels in real time. Notably, we found that the transition from serum/LIF to 2i was accompanied by an unexpectedly rapid downregulation of *Utf1* that was clearly detectable within 24 hr (Figure 4A; Movie S1). Intriguingly, this switch was fully reversible with similar kinetics when cells were switched back from 2i to serum/LIF (Figure 4A; Movie S2). Since the *Utf1* reporter provided us with a simple and sensitive readout, we further explored the effect of the individual inhibitors on this reversible dynamic. As shown in Figure 4B, the downregulation of *Utf1* was largely attributable to the MEK inhibitor, and not the GSK3 $\beta$  inhibitor (Figure 4B). Our study highlights *Utf1* as one of the most dynamically regulated TFs in the two ESC culture conditions.

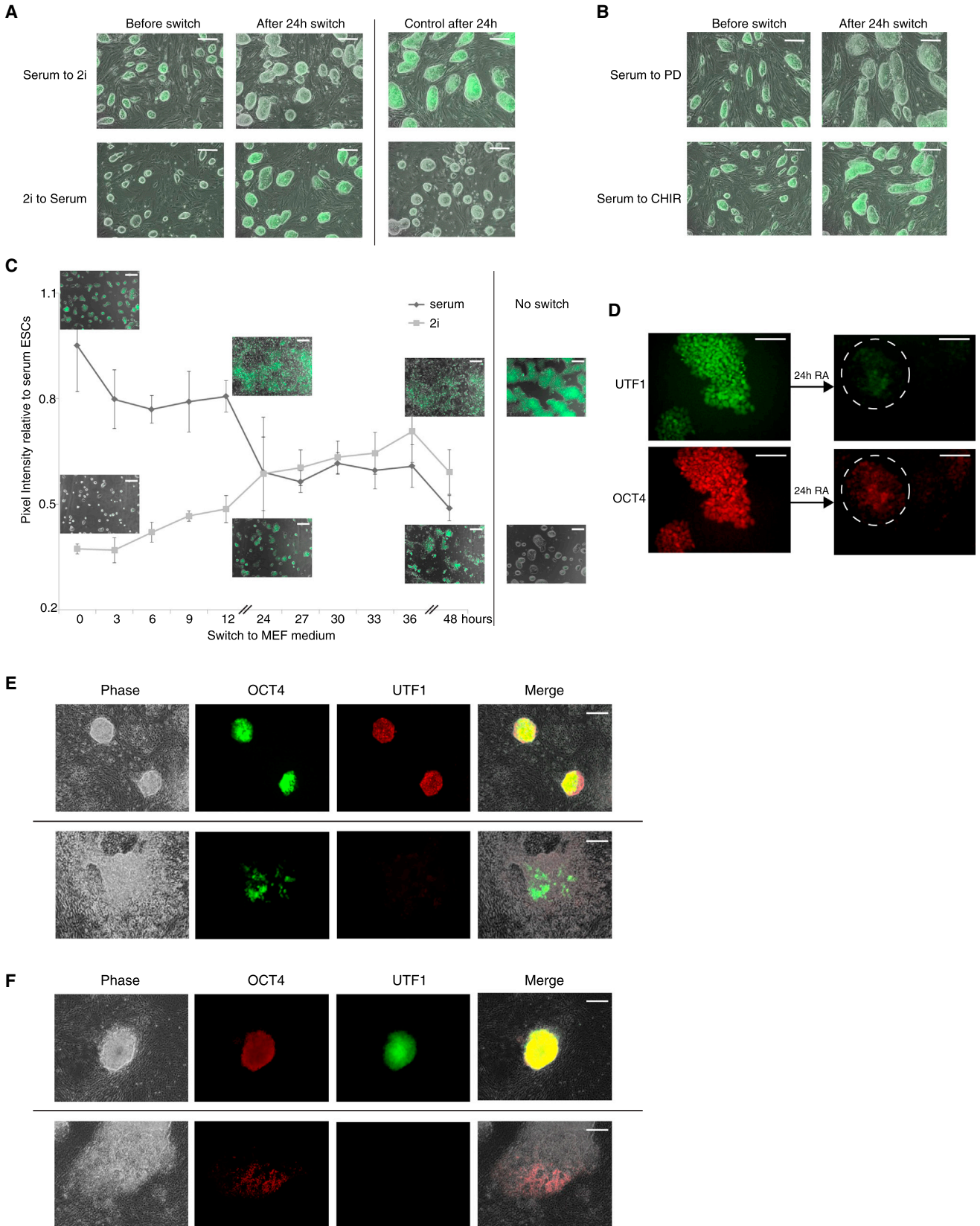
### ***Utf1* Is Downregulated during In Vitro Differentiation and Is Specifically Upregulated in Reprogrammed Cells**

Given the tight regulation of *Utf1* in the two distinct pluripotency conditions, we wanted to further explore its dynamics during differentiation and reprogramming. We first analyzed UTF1 dynamics during undirected differentiation of the CHG1.7 ESCs in both serum/LIF and 2i conditions. To induce differentiation, we switched to serum-containing mouse embryonic fibroblast (MEF) media that was deprived of LIF or the two inhibitors. Interestingly, when starting from the serum condition, we observed a progressive downregulation of the reporter signal accompanied by flattening of the colonies and clear morphological changes associated with differentiation (Figure 4C). In contrast, 2i cells showed transient upregulation of the reporter expression prior to their morphologic differentiation. We confirmed that both UTF1 and OCT4 during retinoic acid (RA)-induced differentiation showed similar trends (Figure 4D). To test whether UTF1 in general and its transient upregulation in 2i conditions are required for the differentiation of mouse ESCs, we generated a *Utf1* knockout cell line (CHG3.70; Figures S4A and S4B) and induced differentiation with RA for 48 hr. To more quantitatively compare the differentiation capacity of knockout and wild-type cells, we used a simple replating assay to test for residual pluripotent cells after induction with RA. Replating the cells on MEFs with serum/LIF media resulted in approximately two times more alkaline phosphatase (AP)-positive cells compared with the control (Figure S4C), suggesting a delayed, but not completely blocked, differentiation potential for *Utf1*-deficient cells. Additionally, *Utf1* knockout cells could contribute to chimeras upon blastocyst injection, which is in accordance with previous reports (Figure S4D; Jia et al., 2012; Nishimoto et al., 2013).

To explore *Utf1* dynamics during reprogramming to pluripotency, we injected the CHG2.4 reporter ESCs into blastocysts and derived *Utf1* reporter MEFs from the resulting chimeras. We then transduced our *Utf1* reporter MEFs along with frequently used *Oct4* reporter MEFs (Szabó et al., 2002) to compare the reactivation kinetics of both loci using equivalent *Oct4*, *Sox2*, *Klf4*, and *Myc* lentiviral titers. Consistent with the literature, we observed the *Oct4* reporter during the onset of induced PSC (iPSC) colony formation around day 9 postinfection. We did not detect any fluorescent signal from the endogenous *Utf1* reporter prior to day 15. Moreover, on day 17 postinfection, we still detected several OCT4-positive cells that appeared partially reprogrammed and could not be propagated upon isolation (Figure 4E). Notably, fully reprogrammed colonies were both OCT4 and UTF1 positive, while OCT4-positive intermediates did not exhibit detectable UTF1 (Figure 4E). Conversely, all UTF1-reporter-positive colonies were OCT4 positive and could be easily propagated in isolation (Figure 4F). Again, partially reprogrammed cells or other subpopulations were found to be positive for OCT4 but negative for UTF1. We next used fluorescence-activated cell sorting (FACS) analysis of CHG2.4 reporter MEFs on day 20 of reprogramming (8 days after doxycycline removal) to quantify the different populations. To this end, we stained cells for OCT4 and compared the fractions of OCT4/UTF1 single-positive versus OCT4/UTF1 double-positive cells. The CHG2.4 MEF control was negative for UTF1 and OCT4 (Figure S4E), while reprogrammed cells could be classified into three categories: a minor fraction of UTF1-only cells, a fraction of OCT4/UTF1 double-positive cells, and a similar fraction of OCT4-only cells (Figure S4F). Similarly to reprogramming in mouse, human fibroblasts showed specific induction of *UTF1* upon successful reprogramming, though with highly variable levels among all pluripotent cells (Figure S4G).

## **DISCUSSION**

Defining and characterizing key regulators of the pluripotency network remains a major task in the stem cell field. *Utf1* is tightly linked to pluripotency, but despite several recent studies, its exact role remains incompletely understood. Here, we report the generation and characterization of two *Utf1* reporter lines and demonstrate their utility for efficient tracking, mapping, and purification of the endogenous UTF1 protein. Our results confirm the dynamic expression of *Utf1* in vivo and in vitro, and show the power of these reporter systems for live-cell imaging. Two findings of particular relevance to the stem cell community are the rapid and reversible downregulation of *Utf1* when ESCs were switched from serum/LIF to 2i, and the late but highly



(legend on next page)



specific upregulation of this factor during reprogramming. The dynamic regulation observed during the switch to 2i not only establishes *Utf1* as a very sensitive marker that distinguishes two LIF-regulated pluripotent states but also suggests that it may be a possible regulator of downstream transcriptional and epigenetic changes (Marks et al., 2012). The reprogramming experiments highlight the utility of *Utf1* as a specific marker for the isolation of fully reprogrammed cells, and suggest that it may facilitate screens for small molecules or additional factors that specifically enhance late-stage transitions from intermediate to fully reprogrammed cells. In summary, the multipurpose design and high specificity of the endogenous *Utf1* reporter system make it a valuable resource that can be specifically applied to address numerous questions in stem cell and developmental biology.

## EXPERIMENTAL PROCEDURES

### Cell Culture and Mice

Mouse ESCs were cultured on irradiated CF1 feeders in DMEM containing 15% fetal bovine serum (FBS), 1% penicillin/streptomycin, 1% glutamine, 1% nonessential amino acid, and  $5 \times 10^5$  U LIF. All mouse work was done according to Harvard University guidelines and approved by the institutional animal care and use committee. 2i medium was prepared as described previously (Ying et al., 2008) and supplemented with  $5 \times 10^5$  U LIF. To induce BirA biotin ligase expression, the culture medium was supplemented with 2  $\mu$ g/ml doxycycline. See [Supplemental Experimental Procedures](#) for more details.

### Antibodies

ChIP was performed at a final concentration of  $1 \mu$ g/ $1 \times 10^6$  cells with UTF1 (ab24273; Abcam). Immunostaining was done with the following primary antibodies (all diluted 1:1,000): UTF1

(ab24273; Abcam), OCT4 (611202; BD), and NANOG (560259; BD). Western blots were done using the following antibodies: histone H3 (1:5,000; ab61251; Abcam), and biotin (horseradish peroxidase-conjugated streptavidin 1:5,000, N-100; Thermo Scientific).

### TALEN Assembly

TALEN assembly was performed according to a previously described protocol (Ding et al., 2013).

### ChIP and Biotin Pulldown

Cells were crosslinked in 1% formaldehyde for 5 min at room temperature, with constant agitation, followed by quenching with 125 mM glycine for 5 min. Immunoprecipitation was done as previously described (Mikkelsen et al., 2010). For bioChIP, streptavidin-coupled Dynabeads (Invitrogen) were incubated with chromatin for 2–3 hr at 4°C. The SDS concentration in low-salt buffer was raised to 2% and reverse crosslinking was performed on beads overnight at 65°C.

### Cellular Reprogramming

E14.5 MEFs were generated as previously described (Koche et al., 2011). Oct4-GFP MEFs were generated from the B6;CBA-Tg(Pou5f1-EGFP)2Mnn/J strain (The Jackson Laboratory). Passage 2 MEFs were seeded at a density of 200,000 cells/10 cm<sup>2</sup> dish. The next day, cells were infected with FUW lentivirus harboring the *Oct4*, *Sox2*, *Myc*, *Klf4*, or rtTA open reading frame. One day postinfection the medium was changed to serum/LIF medium, and 2 days postinfection the medium was supplemented with 2  $\mu$ g/ml doxycycline. Twelve days postinfection, doxycycline was removed from the culture. Images were taken 17 days postinfection.

### ACCESSION NUMBERS

The ChIP-seq data have been deposited in the Gene Expression Omnibus under accession number GSE53768.

## Figure 4. *Utf1* in Pluripotency, Differentiation, and Reprogramming

(A) The *Utf1* fusion line CHG1.7 was switched for 24 hr from serum/LIF to 2i or for 24 hr from 2i to serum/LIF. The switch to 2i results in a rapid downregulation of UTF1 levels. Conversely, the switch to serum/LIF induces a rapid upregulation of UTF1. Scale bar, 150  $\mu$ m. Exposure times are consistent between the different images.

(B) Individual effect of the MEK or GSK3 $\beta$  inhibitor on UTF1 levels. Scale bar, 150  $\mu$ m. Exposure times are consistent between the different images.

(C) Undirected differentiation of CHG1.7 starting from serum/LIF or 2i culture conditions. ESCs cultured in serum/LIF prior to differentiation exhibit a progressive downregulation of the fluorescent reporter concomitantly with flattening and differentiation of the colonies. Cells cultured in 2i prior to differentiation upregulate the reporter in the first 36 hr and display delayed morphological differentiation. Scale bar, 150  $\mu$ m. Whiskers show 1 SD for n = 3 independent experiments.

(D) RA-induced differentiation for 24 hr using CHG1.7. Both UTF1 and OCT4 (immunostaining) show rapid downregulation in response to RA. Scale bar, 100  $\mu$ m.

(E) Cellular reprogramming (day 17 after transgene induction) of *Oct4* reporter MEFs. Fully reprogrammed colonies are positive for both OCT4 and UTF1 (immunostaining); however, partially reprogrammed cells or other subpopulations were only found to be positive for OCT4. Scale bar, 150  $\mu$ m.

(F) Cellular reprogramming (day 17 after transgene induction) of *Utf1* mCitrine reporter MEFs. Fully reprogrammed colonies were positive for UTF1 and OCT4 (immunostaining); however, partially reprogrammed cells or other subpopulations were again only found to be positive for OCT4. Scale bar, 150  $\mu$ m.

See also [Figure S4](#).



## SUPPLEMENTAL INFORMATION

Supplemental Information includes Supplemental Experimental Procedures, four figures, and two movies and can be found with this article online at <http://dx.doi.org/10.1016/j.stemcr.2014.01.007>.

## ACKNOWLEDGMENTS

We thank Ramona Pop for help with the FACS, Michael Ziller and Rahul Karnik for help with the data analysis, and Kiran Musunuru for providing the TALEN system and advice regarding its implementation. A.M. is a New York Stem Cell Foundation, Robertson Investigator. This work was funded by the Human Frontiers Science Program and NIH grants 1P50HG006193 and P01GM099117.

Received: September 9, 2013

Revised: January 15, 2014

Accepted: January 16, 2014

Published: February 20, 2014

## REFERENCES

- Apostolou, E., Ferrari, F., Walsh, R.M., Bar-Nur, O., Stadtfeld, M., Cheloufi, S., Stuart, H.T., Polo, J.M., Ohsumi, T.K., Borowsky, M.L., et al. (2013). Genome-wide chromatin interactions of the Nanog locus in pluripotency, differentiation, and reprogramming. *Cell Stem Cell* *12*, 699–712.
- Barker, D.F., and Campbell, A.M. (1981). The *birA* gene of *Escherichia coli* encodes a biotin holoenzyme synthetase. *J. Mol. Biol.* *146*, 451–467.
- Beard, C., Hochedlinger, K., Plath, K., Wutz, A., and Jaenisch, R. (2006). Efficient method to generate single-copy transgenic mice by site-specific integration in embryonic stem cells. *Genesis* *44*, 23–28.
- Buganim, Y., Faddah, D.A., Cheng, A.W., Itskovich, E., Markoulaki, S., Ganz, K., Klemm, S.L., van Oudenaarden, A., and Jaenisch, R. (2012). Single-cell expression analyses during cellular reprogramming reveal an early stochastic and a late hierarchic phase. *Cell* *150*, 1209–1222.
- de Wit, E., Bouwman, B.A., Zhu, Y., Klous, P., Splinter, E., Verstegen, M.J., Krijger, P.H., Festuccia, N., Nora, E.P., Welling, M., et al. (2013). The pluripotent genome in three dimensions is shaped around pluripotency factors. *Nature* *501*, 227–231.
- Ding, Q., Lee, Y.K., Schaefer, E.A., Peters, D.T., Veres, A., Kim, K., Kuperwasser, N., Motola, D.L., Meissner, T.B., Hendriks, W.T., et al. (2013). A TALEN genome-editing system for generating human stem cell-based disease models. *Cell Stem Cell* *12*, 238–251.
- Jaenisch, R., and Young, R. (2008). Stem cells, the molecular circuitry of pluripotency and nuclear reprogramming. *Cell* *132*, 567–582.
- Jia, J., Zheng, X., Hu, G., Cui, K., Zhang, J., Zhang, A., Jiang, H., Lu, B., Yates, J., 3rd, Liu, C., et al. (2012). Regulation of pluripotency and self-renewal of ESCs through epigenetic-threshold modulation and mRNA pruning. *Cell* *151*, 576–589.
- Kim, J., Chu, J., Shen, X., Wang, J., and Orkin, S.H. (2008). An extended transcriptional network for pluripotency of embryonic stem cells. *Cell* *132*, 1049–1061.
- Koche, R.P., Smith, Z.D., Adli, M., Gu, H., Ku, M., Gnirke, A., Bernstein, B.E., and Meissner, A. (2011). Reprogramming factor expression initiates widespread targeted chromatin remodeling. *Cell Stem Cell* *8*, 96–105.
- Kooistra, S.M., van den Boom, V., Thummer, R.P., Johannes, F., Wardenaar, R., Tesson, B.M., Veenhoff, L.M., Fusetti, F., O'Neill, L.P., Turner, B.M., et al. (2010). Undifferentiated embryonic cell transcription factor 1 regulates ESC chromatin organization and gene expression. *Stem Cells* *28*, 1703–1714.
- Marks, H., Kalkan, T., Menafrá, R., Denissov, S., Jones, K., Hofmeister, H., Nichols, J., Kranz, A., Stewart, A.F., Smith, A., and Stunnenberg, H.G. (2012). The transcriptional and epigenomic foundations of ground state pluripotency. *Cell* *149*, 590–604.
- Mikkelsen, T.S., Xu, Z., Zhang, X., Wang, L., Gimble, J.M., Lander, E.S., and Rosen, E.D. (2010). Comparative epigenomic analysis of murine and human adipogenesis. *Cell* *143*, 156–169.
- Ng, H.H., and Surani, M.A. (2011). The transcriptional and signaling networks of pluripotency. *Nat. Cell Biol.* *13*, 490–496.
- Nishimoto, M., Katano, M., Yamagishi, T., Hishida, T., Kamon, M., Suzuki, A., Hirasaki, M., Nabeshima, Y., Nabeshima, Y., Katsura, Y., et al. (2013). In vivo function and evolution of the eutherian-specific pluripotency marker UTF1. *PLoS ONE* *8*, e68119.
- Okuda, A., Fukushima, A., Nishimoto, M., Orimo, A., Yamagishi, T., Nabeshima, Y., Kuro-o, M., Nabeshima, Y., Boon, K., Keaveney, M., et al. (1998). UTF1, a novel transcriptional coactivator expressed in pluripotent embryonic stem cells and extra-embryonic cells. *EMBO J.* *17*, 2019–2032.
- Szabó, P.E., Hübner, K., Schöler, H., and Mann, J.R. (2002). Allele-specific expression of imprinted genes in mouse migratory primordial germ cells. *Mech. Dev.* *115*, 157–160.
- Takahashi, K., and Yamanaka, S. (2006). Induction of pluripotent stem cells from mouse embryonic and adult fibroblast cultures by defined factors. *Cell* *126*, 663–676.
- van den Boom, V., Kooistra, S.M., Boesjes, M., Geverts, B., Houtsmuller, A.B., Monzen, K., Komuro, I., Essers, J., Drenth-Diephuis, L.J., and Eggen, B.J. (2007). UTF1 is a chromatin-associated protein involved in ES cell differentiation. *J. Cell Biol.* *178*, 913–924.
- Ying, Q.L., Nichols, J., Chambers, I., and Smith, A. (2003). BMP induction of Id proteins suppresses differentiation and sustains embryonic stem cell self-renewal in collaboration with STAT3. *Cell* *115*, 281–292.
- Ying, Q.L., Wray, J., Nichols, J., Batlle-Morera, L., Doble, B., Woodgett, J., Cohen, P., and Smith, A. (2008). The ground state of embryonic stem cell self-renewal. *Nature* *453*, 519–523.
- Zhao, Y., Yin, X., Qin, H., Zhu, F., Liu, H., Yang, W., Zhang, Q., Xiang, C., Hou, P., Song, Z., et al. (2008). Two supporting factors greatly improve the efficiency of human iPSC generation. *Cell Stem Cell* *3*, 475–479.